Properties of A Supercritical Quasi-Perpendicular Interplanetary Shock Propagating in Super-Alfvénic Solar Wind: from MHD to Kinetic Scales

Mingzhe Liu, Zhongwei Yang, D. Liu Ying, Bertrand Lembège, Karine Issautier, Lynn Bruce Wilson Iii, Siqi Zhao, Vamsee Krishna Jagarlamudi, Xiaowei Zhao

Properties of A Supercritical Quasi-Perpendicular Interplanetary Shock Propagating in Super-Alfvénic Solar Wind: from MHD to Kinetic Scales

Mingzhe Liu[1,2,3], Zhongwei Yang[2], Ying D. Liu[2,4], Bertrand Lembège[3], Karine Issautier[1], L. B. Wilson III[5], Siqi Zhao[6], Vamsee Krishna Jagarlamudi[7], Xiaowei Zhao[2]

1. LESIA, Observatoire de Paris, Université PSL, CNRS, 92195, Meudon, France; mingzhe.liu@obspm.fr;
2. State Key Laboratory of Space Weather, NSSC, CAS, Beijing 100190, China
3. LATMOS/IPSL, UVSQ Paris-Saclay University, Sorbonne University, CNRS, Guyancourt, France
4. University of Chinese Academy of Sciences, Beijing 100049, China
5. NASA Goddard Space Flight Center, Code 672, Greenbelt, Maryland, MD20707, USA
6. Deutsches Elektronen Synchrotron (DESY), Platanenallee 6, D-15738 Zeuthen, Germany
7. National Institute for Astrophysics- Institute for Space Astrophysics and Planetology, 00133 Roma, Italy

EGU21-4908

1. Abstract

We investigate the properties of an interplanetary shock (M_A=3.0, θ_{Bn}=80°) propagating in Super-Alfvénic solar wind observed on September 12th 1999 with *in situ* **Wind/MFI** and **Wind/3DP** observations. Key results are obtained concerning the possible energy dissipation mechanisms across the shock and how the shock modifies the ambient solar wind at MHD and kinetic scales: (1) Waves observed in the far upstream of the shock are incompressional and mostly shear Alfvén waves. (2) In the downstream, the shocked solar wind shows both Alfvénic and mirror-mode features due to the coupling between the Alfvén waves and ion mirror-mode waves. (3) Specularly reflected gyrating ions, whistler waves, and ion cyclotron waves are observed around the shock ramp, indicating that the shock may rely on both particle reflection and wave-particle interactions for energy dissipation. (4) Both ion cyclotron and mirror mode instabilities may be excited in the downstream of the shock, since the proton temperature anisotropy touches their thresholds due to the enhanced proton temperature anisotropy. (5) Whistler heat flux instabilities excited around the shock give free energy for the whistler precursors, which help explain the isotropic electron number and energy flux together with the normal betatron acceleration of electrons across the shock. (6) The shock may be somehow connected to the electron foreshock region of the Earth's bow shock, since $B_x > 0$, $B_y < 0$, and the electron flux varies only when the electron pitch angles are less than PA = 90°, which should be further investigated.

2. Research background and motivations

2.1 Research background

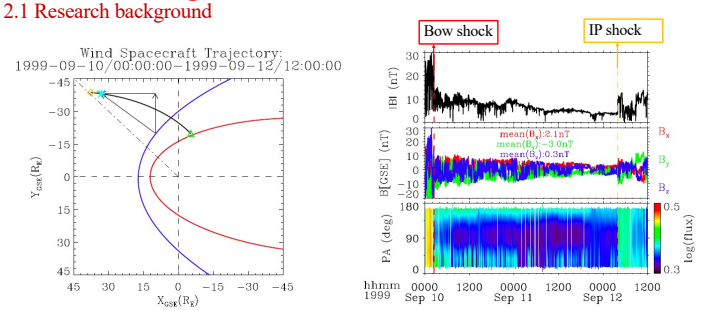

Fig 1: (Left) Wind Satellite orbit (green) with empirical model bow shock (blue, see Peredo et al., 1995) and magnetopause (red, see Roelof & Sibeck., 1993) plotted for reference. The triangle and diamond respectively represent the start and end of Wind trajectory. The asterisk denotes the position where an IP shock was detected by Wind. (Right) The Wind observations which corresponds to the trajectory shown in the left. From top to bottom, the panels show the magnetic field magnitude, GSE components of the magnetic field, pitch-angle distribution of 340 eV electrons.

- IP Shock Information Obtained from SDAT (Vinas & Scudder 1986).
  - (1) M_f=2.1 & M_A=3.0: Supercritical; θ_{Bn}=80 deg: Quasi-perpendicular;
  - (2) |B| increases across the shock: Fast shock; V_{shn}=532.8 km/s > V_p : Forward shock.
- The IP shock was immersed in the quasi-parallel region of the Earth's bow shock.
  - (1) Time: 03:57:56 UT on September 12th, 1999
  - (2) Location: GSE (33.1, -38.1, -3.9) R_E; To the Earth's bow shock: ~34.0 R_E.

2.2 Motivations

- When IP shocks are Earth–directed, how IP shock interact with the foreshock region of Earth's bow shock? Mutual affectation on each other.
- Alfvén waves/fluctuations are usually observed in the foreshock region of Earth's bow shock (eg., Wang et al., 2015 and references therein): Properties of IP shock propagating in the high-Alfvénic solar wind.
- The properties of the bow-shock-reflected electrons and how they are affected by the IP shock.

3. Observations and results

3.1 Overview and MHD properties of the IP shock

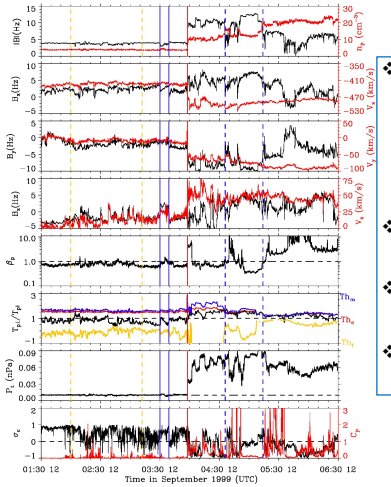

- Alfvén waves/fluctuations: (1) $V_{x,y,z}$ in phase with $B_{x,y,z}$; (2) σ_c close to 1.

$$\sigma_c(t) = \frac{2\langle d\mathbf{V}\cdot d\mathbf{V}_b\rangle}{\langle d\mathbf{V}\cdot d\mathbf{V}\rangle + \langle d\mathbf{V}_b\cdot d\mathbf{V}_b\rangle}$$

$$C_p(t) = \frac{\langle dN_p^2\rangle}{\overline{N_p}^2}\,\frac{\overline{B}^2}{\langle d\mathbf{B}\cdot d\mathbf{B}\rangle}$$

- IP shock modifies the Alfvén wave propagation direction.
- In downstream of IP shock, ion cyclotron and mirror mode instabilities may be excited.
- In the upstream of IP shock, $B_x > 0$, $B_y < 0$: B direct to the Sun.

Fig 2: Solar wind measurements around the 1999 September the 12th shock event from Wind. From top to bottom, the panels show the comparison between magnetic field strength and proton number density, the comparison between X (Y, Z) component of magnetic field and proton bulk velocity in Geocentric Solar Ecliptic (GSE) coordinates, plasma β_p, the ratio of the perpendicular temperature to the parallel temperature with thresholds of ion cyclotron (red), mirror-mode (blue) and firehose (yellow) instabilities for comparison, the total plasma pressure (proton thermal pressure plus magnetic pressure), and the comparison between cross–helicity and the compressibility, respectively. The red vertical line marks the shock propagating in the the ambient solar wind. The region denoted by two blue dashed vertical lines in the downstream of the shock are mirror mode wave structures.

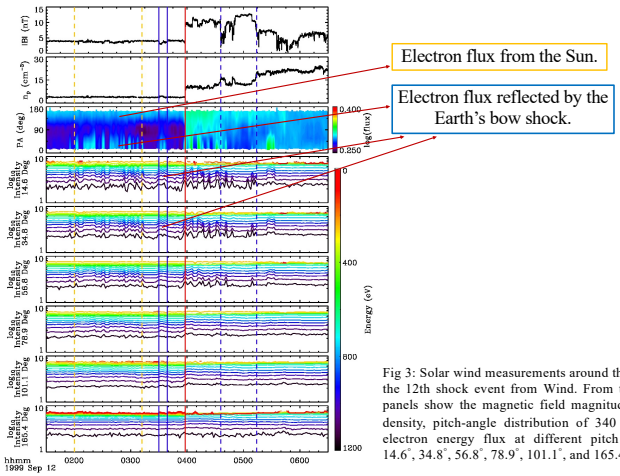

Fig 3: Solar wind measurements around the 1999 September the 12th shock event from Wind. From top to bottom, the panels show the magnetic field magnitude, proton number density, pitch-angle distribution of 340 eV electrons and electron energy flux at different pitch angles including 14.6°, 34.8°, 56.8°, 78.9°, 101.1°, and 165.4°.

3.2 Kinetic analysis

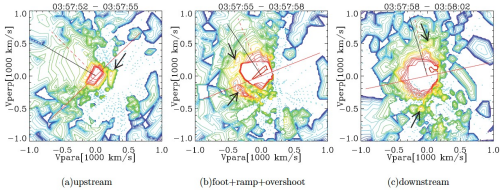

Fig 4: Evolution of the ion distributions (in the solar wind frame) across the shock ramp obtained from the 3DP/PESA-High instruments. Projected onto the planes are the following: shock normal direction (dashed red line), shock surface (solid red line), and solar wind velocity direction (solid black line).

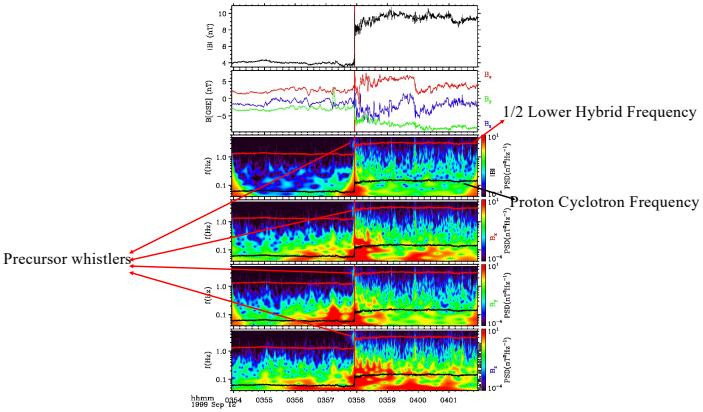

Fig 5: Wavelet analysis of the magnetic measurements around the 1999 September the 12th shock case. From top to bottom, the panels show the magnetic field magnitude, GSE components of the magnetic field, wavelet analysis of magnetic field magnitude |B| and components including B_x, B_y and B_z respectively.

Time(UT)	$T_{\perp e}/T_{\parallel e}$	$T_{\perp h}/T_{\parallel h}$	$T_{\parallel h}/T_{\parallel e}$	$\beta_{\parallel e}$	n_{ce}(cm^{-3})	n_{he}(cm^{-3})	n_{he}/n_{ce}
03:57:49–03:57:52	0.71	0.65	9.85	1.61	3.61	0.27	0.075
03:57:52–03:57:55	0.72	0.89	6.90	1.67	2.27	0.20	0.087
03:57:55–03:57:58	1.10	1.09	7.56	0.84	4.27	0.27	0.063
03:57:58–03:58:02	1.03	1.10	10.31	1.10	7.35	0.10	0.014
03:58:02–03:58:05	0.98	1.07	10.31	1.23	7.20	0.10	0.015

Table 1: Wind/3DP Electron Parameters from EESA-Low Burst Mode Data.

Whistler heat flux instabilities

(1)Unstable when $T_{\perp h}/T_{\parallel h} > 1.01$;

(2)Stable when $\beta_{\parallel e} \leqslant 0.25$.

4. Discussion and perspective

- ✓ Starting from the Earth's bow shock, its electron foreshock region can reach more than 34 R_E.
- ✓ The electrons coming from both the Sun and the Earth's bow shock are pitch-angle scattered across the shock by both the whistler heat flux instabilities and normal betatron acceleration.
- ✓ The IP shock modifies the properties of the waves/fluctuation at the Earth's foreshock region (eg., propagation direction, compression ……).
- ✓ The evolution of the turbulence across the IP shock needs to be further investigated.